Article

The Role of Trichloroacetimidate To Enable Iridium-Catalyzed Regio- and Enantioselective Allylic Fluorination: A Combined Experimental and Computational Study

Alexandre M. Sorlin, Jason C. Mixdorf, Madeline Rotella, Robert Martin, Osvaldo Gutierrez, and Hien M. Nguyen

J. Am. Chem. Soc., **Just Accepted Manuscript** • DOI: 10.1021/jacs.9b07575 • Publication Date (Web): 22 Aug 2019

The Role of Trichloroacetimidate To Enable Iridium-Catalyzed Regio- and Enantioselective Allylic Fluorination: A Combined Experimental and Computational Study

Alexandre M. Sorlin,[†,1,#] *Jason C. Mixdorf,*[†,1,#] *Madeline E. Rotella,*[†,2,#] *Robert T. Martin,*[2#] *Osvaldo Gutierrez*[*,2,#] *and Hien M. Nguyen*[*,3,#]

[1]Department of Chemistry, University of Iowa, Iowa City, Iowa 52242, United Sates

[2]Department of Chemistry and Biochemistry, University of Maryland, College Park, Maryland 20742, United States

[3]Department of Chemistry, Wayne State University, Detroit, Michigan 48202, United States

Email: ogs@umd.edu and hmnguyen@wayne.edu

ABSTRACT

Asymmetric allylic fluorination has proven to be a robust and efficient methodology with potential applications for the development of pharmaceuticals and practical synthesis for ^{18}F-radiolabeling. A combined computational (dispersion corrected-DFT) and experimental approach was taken to interrogate the mechanism of the diene-ligated iridium-catalyzed regio- and enantioselective allylic fluorination. Our group has shown that in the presence of an iridium(I) catalyst and nucleophilic fluoride source ($Et_3N{\bullet}3HF$), allylic trichloroacetimidates undergo rapid fluoride substitution to generate allylic fluoride products with excellent levels of branched-to-linear ratios. Mechanistic studies reveal the crucial role of the trichloroacetimidate as a potent leaving group and ligand to enable

conversion of racemic allylic trichloroacetimidates to the corresponding enantioenriched allylic fluorides, via a dynamic kinetic asymmetric transformation (DYKAT), in the presence of the chiral bicyclo[3.3.0]octadiene-ligated iridium catalyst.

INTRODUCTION

The trichloroacetimidate functional group has been utilized in a wide range of synthetic chemistry. Pioneered by Schmidt as an efficient leaving group in carbohydrate glycosylation reactions,[1-4] the trichloroacetimidate was further used by Overman in selective [3,3]-sigmatropic rearrangements forming allylic trichloroacetamides.[5-6] It has been recently reported that trichloroacetimidates have broad utility in allylic substitution for the creation of C-N, C-O, and C-F bonds.[7] One of the synthetic utilities of trichloroacetimidates is highlighted in the transition-metal-catalyzed substitution to generate allylic fluorides,[8-9] which can serve as valuable scaffolds for construction of pharmaceuticals,[10-15] medicinal imaging tracers,[16] and agrochemicals.[17-18] Although there have been several efficient methodologies reported for the regioselective formation of allylic fluorides,[19-25] there are few approaches available for the asymmetric synthesis of allyl fluorides.[9, 26-29] In 2011, initial studies toward a regioselective fluorination reaction were undertaken in our group. Accordingly, allylic trichloroacetimidates **1** were employed as electrophiles, Et_3N•3HF as a nucleophilic fluoride source, and cyclooctadiene iridium chloride dimer, $[Ir(COD)Cl]_2$, as a catalyst leading to the formation of branched allylic fluorides **2** in good yields and excellent regioselectivities (Scheme 1a).[8] In subsequent studies, racemic secondary allylic trichloroacetimidates **3** were transformed to enantioenriched allylic fluorides **4** catalyzed by a chiral bicyclo[3.3.0]octadiene (*S,S*)-ligated iridium complex (Scheme 1b).[9, 29]

Scheme 1. Selective allylic C-F bond formation

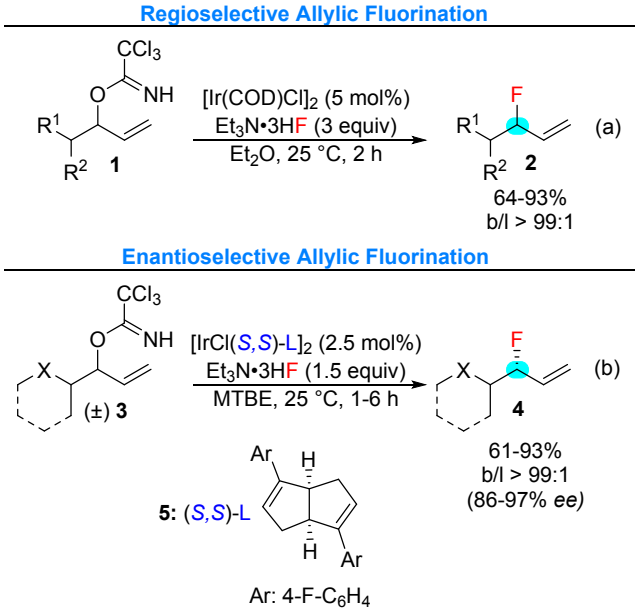

Herein, we report a detailed investigation that provides insight into the mechanism and origin of regio- and enantioselectivity of the iridium-catalyzed allylic fluorination. Overall, a synergistic computational and experimental study provides strong support for a dynamic kinetic asymmetric transformation (DYKAT) of racemic allylic trichloroacetimidate, leading to regio- and enantioselective allylic C-F bond formation. This combined study also highlights the dualistic nature of the trichloroacetimidate as a leaving/directing group and as a ligand to facilitate equilibration of diastereomeric π-allyl iridium intermediates via a π-σ-π mechanism, leading to enantioenriched allylic fluorides.

RESULTS AND DISCUSSION

Based on previous work focused on transition-metal-catalyzed allylic substitutions,[30-34,35-42] a general scheme for iridium-catalyzed allylic fluorination could be hypothesized (Scheme 2). First, allylic trichloroacetimidate **A** coordinates with [Ir] catalyst then undergoes ionization of the C-O bond leading to the formation of π-allyl iridium intermediate **B**. The π-allyl iridium complex **B** is proposed to react with nucleophilic fluoride, resulting in allylic fluoride product **C**.

Scheme 2. Proposed intermediate steps for the iridium-catalyzed allylic fluorination

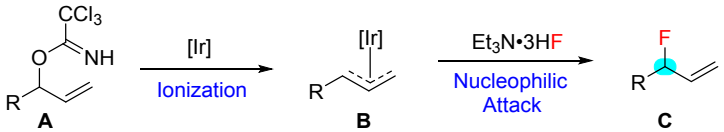

To gain insight into the unique features of the trichloroacetimidate to promote iridium-catalyzed regio- and enantioselective allylic fluorination, dispersion-corrected DFT calculations were performed (see Supporting Information for full computational methods). To

reduce computational cost, allylic trichloroacetimidate **6** (Scheme 3) was used as the model substrate for all calculations. *To validate the use of this model substrate*, a subsequent experiment was performed (Scheme 3) to ensure that this trichloroacetimidate **6** also provided the allylic fluoride product with excellent levels of regioselectivity. As illustrated in Scheme 3, subjection of substrate **6** to the standard fluorination conditions provided the desired allylic fluoride **7** with branched-to-linear ratios greater than 99:1, therefore, validating the use of substrate **6** for computational studies.

Scheme 3. Fluorination of model substrate **6**

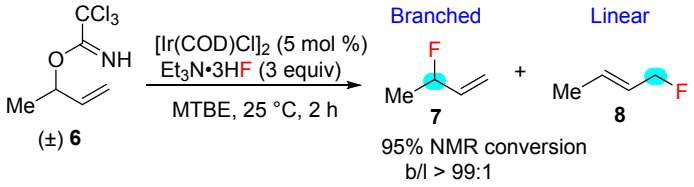

Using this model system, the mechanism of iridium-catalyzed allylic fluorination was then investigated (for information on the choice of the computational method, see Figure S1 in the Supporting Information). First, the most energetically favored mode of complexation between allylic trichloroacetimidate **6** and $[Ir(COD)Cl]_2$, presumably resulting from fragmentation of dimeric $[Ir(COD)Cl]_2$ pre-catalyst, was explored.[43-48] After extensive conformational analysis (see Figure S2 in the Supporting Information) and exploration of various modes of coordination, three distinct isomeric structures were identified (Figure 1). Overall, calculations revealed a strong energetic preference for bidentate coordination to the allylic trichloroacetimidate substrate via η^2-(π-coordination) of the olefin and η^1-(σ-coordination) to the nitrogen atom of the imine group, to form a pentacoordinated square pyramidal **6-Ir-A** complex. Monodentate coordination to either imine or olefin to form tetracoordinated square planar complexes **6-Ir-B** and **6-Ir-C** are > 6 kcal/mol higher in energy. Presumably, the strong ability of the imine and olefin to coordinate in a bidentate fashion overcomes strain associated with forming the 7-member chelated complex **6-Ir-A**.[49] We postulate that this mode of coordination (i.e., **6-Ir-A**) is crucial for reactivity as it pre-organizes the catalyst-substrate complex for facile C-O bond breaking (i.e., lowest energetic barrier for ionization is 8.7 kcal/mol leading to π-allyl iridium intermediate **6-Ir-D**, downhill in energy by 10.7 kcal/mol; for other competing pathways see Figure S4 in the Supporting Information). A distortion-interaction analysis is provided in the Supporting Information (see Figure S5) to better understand the reactivity and, in particular, why the ionization via the 7-member chelated complex (6-Ir-A) is much lower in energy than the alternatives.

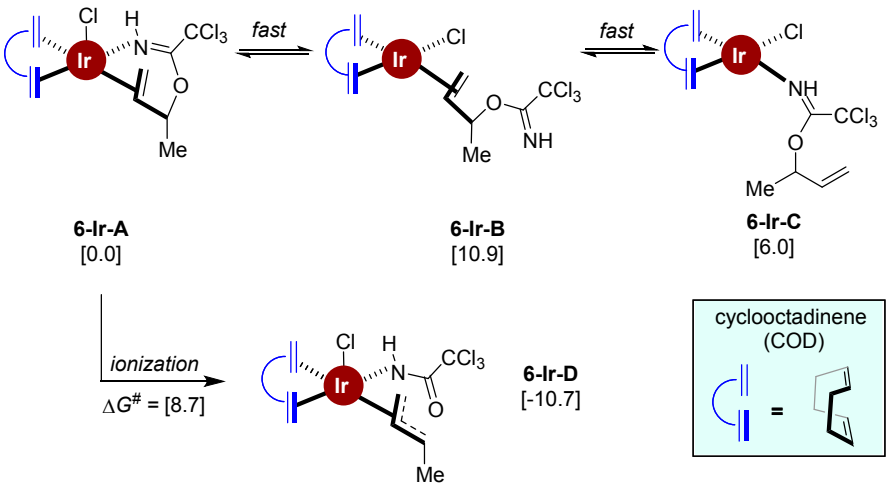

Figure 1. Identification of various modes of iridium coordination to allylic trichloroacetimidates. Free energies (kcal/mol) were computed using B3LYP-D3/6-311+G(d,p)-SDD(Ir)-CPCM (diethyl ether)//M06/6-31G(d,p)-LANL2DZ (Ir)-CPCM (diethyl ether) in brackets.

To test the hypothesis that **6-Ir-D** complex is an active intermediate in the reaction, we subsequently mixed allylic trichloroacetimidate (*R*)-**9** with $[Ir(COD)Cl]_2$ catalyst **10** (Figure 2).[50] A white precipitate was isolated and further characterized by X-ray crystallography, confirming a pentacoordinated π-allyl Ir(III) species **11** with η^1-(σ-coordination) of the trichloroacetamide nitrogen to the iridium, which presumably arises from facile ionization of the bidentate Ir-substrate complex (e.g., **6-Ir-A**; Figure 1[51]). Notably, examination of the orientation of the iridium from π-allyl iridium complex shows a retention in stereochemistry from trichloroacetimidate (*R*)-**9**. This evidence supports that the trichloroacetimidate is crucial to induce ionization and acts as both a leaving group and a ligand to the iridium.

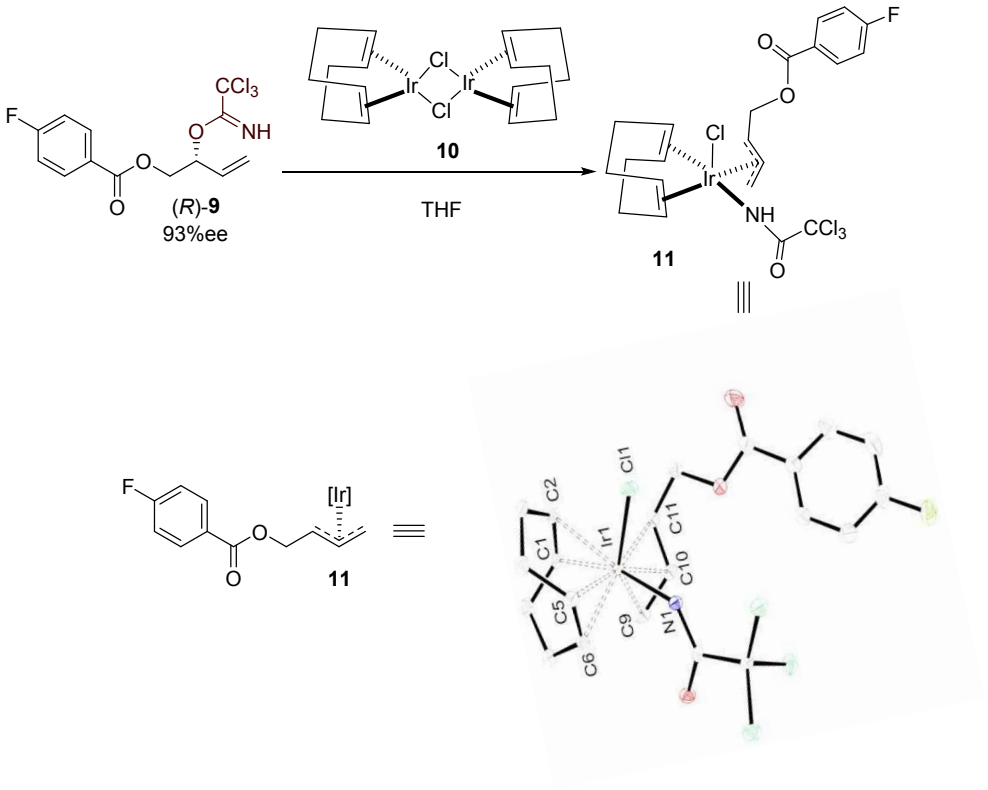

Figure 2. X-ray crystal structure of distorted square pyramidal π-allyl iridium intermediate **11**. Thermal ellipsoids are shown at 50% probability; hydrogen atoms are omitted for clarity. Gray, green, white, blue, red and yellow ellipsoids represent C, Cl, Ir, N, O, and F atoms respectively.

Next, as part of our initial investigation, we examined the effect of the leaving group in the iridium-catalyzed allylic fluorination by subjecting different electrophiles (trichloroacetimidate **9**, acetate **13**, carbonate **14,** and phosphate **16**) to the optimized reaction conditions (Scheme 4). Therein, we found that the use of allylic trichloroacetimidate **9** provided allylic fluoride **12** in 93% yield with branched-to-linear ratios greater than 99:1 (Scheme 4a). In stark contrast, allylic acetate **13** was ineffective toward allylic fluorination formation leading to quantitative recovery of starting material **13** (Scheme 4b). Interestingly, allylic carbonate **14,** which is known to form π-allyl iridium intermediates with cationic character was less reactive towards allylic fluorination (only 10% yield), but formed the undesired allyl ether product **15** (Scheme 4c) as the major product.[52-53] The formation of **15** supports the cationic π-allyl iridium intermediate as methoxide counter anion can be formed after decarboxylation via ionization and acting as nucleophile.[53] In comparison the allylic trichloroacetimidate byproduct, trichloroacetamide, does not act as a nucleophile competing with fluoride attack. Allylic phosphate **16** proceeded smoothly to the regioselective product albeit in lower yield.[54] Given the presumed distinct abilities of the imine of the trichloroacetimidate group to bind to the metal center to form a neutral iridium intermediate, these results further support our hypothesis that the mode of complexation (i.e., **6-Ir-A**, Figure 1) could be essential in the effectiveness of the reaction (*vide supra*). Indeed, computations show that only the trichloroacetimidate substrate favors bidentate coordination while other leaving groups favored monodentate coordination (see Figure S6 for a summary of these results and Figures S7 – S8 in the Supporting Information for details on the conformational search). Since other allylic

substitutions using iridium have been established to proceed with the conservation of stereochemistry in the products,[40, 55-56] could the use of trichloroacetimidate change the stereochemical outcome of allylic substitution?

Scheme 4. Leaving group comparison

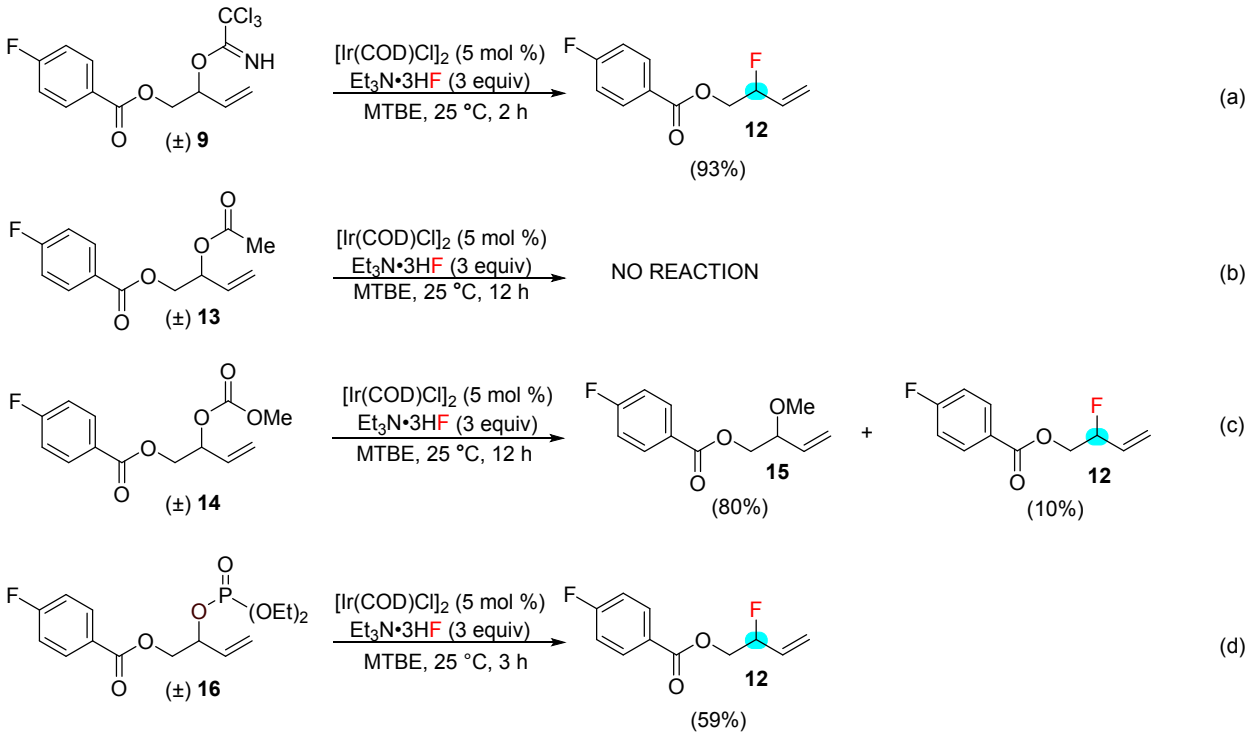

To clarify the stereochemical outcome of our allylic fluorination process, enantioenriched (*S*)-**9** or (*R*)-**9** trichloroacetimidates were subjected to the optimized reaction conditions using $[Ir(COD)Cl]_2$ catalyst (Scheme 5). Each of the enantioenriched (*S*)-**9** or (*R*)-**9** substrates led to nearly racemic (±2% *ee*) allylic fluoride **12** at high conversion. These results attest to the difference between the trichloroacetimidate and other commonly used leaving groups in allylic substitutions as the conservation of the stereochemistry was not observed.[50-51] It has been well-established that η^3-allyl metal complexes can undergo interconversion through a π-σ-π mechanism.[57-58] As such, through conformational analysis on various η^3-allyl iridium intermediates (see Figures S9– S14 in the Supporting Information), we found several isomeric η^3-bound π-allyl iridium complexes that are nearly isoenergetic. Assuming facile π-allyl isomerization, these DFT calculations predict that η^3-bound π-allyl iridium intermediates can quickly equilibrate under experimental conditions. As previously reported, the addition of additives (halide anion or phosphine) to the metal center can increase the rate of isomerization of π-allyl metal intermediates as formation of the sigma complex becomes favored. [59-60] The nature of trichloroacetimidate as a ligand to allow the formation of neutral pentacoordinated π-allyl iridium (III) intermediate could play a key role in the interconversion of π-allyl isomerization and explain racemization of the allylic fluoride product using achiral $[Ir(COD)Cl]_2$ catalyst (Scheme 5).

Scheme 5. Fluorination of enantioenriched allylic trichloroacetimidate substrates

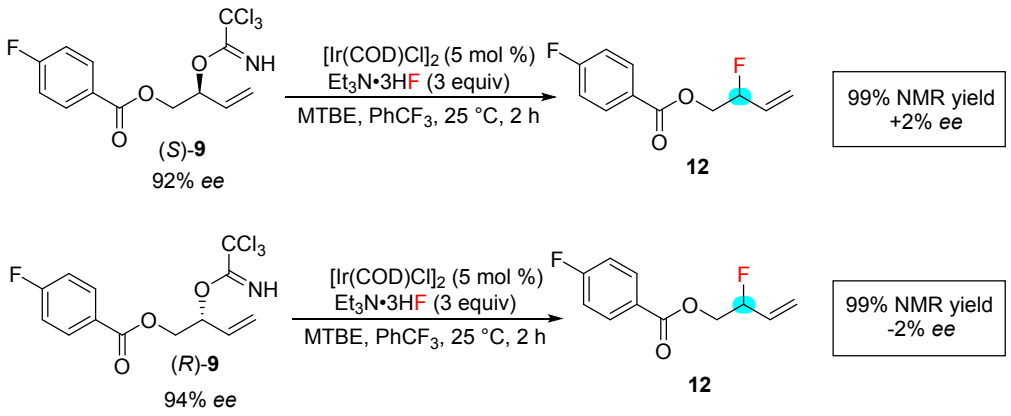

The experimental and computational data leading to the racemic allylic fluoride from enantioenriched starting material suggests that racemic allylic trichloroacetimidate could be converted to a single stereoisomer through a dynamic kinetic asymmetric transformation (DYKAT).[32, 61-62] To probe this hypothesis, racemic allylic trichloroacetimidate **9** was fluorinated using [IrCl(*R*,*R*)-**L**]$_2$ and [IrCl(*S*,*S*)-**L**]$_2$ complexes (**L** = bicyclo[3.3.0]octadiene, Scheme 6). The desired (*R*)- and (*S*)-allylic fluoride products **12** were obtained in good yields and with excellent enantioselectivities (Scheme 6). The absolute stereochemistry of **12** was established via X-ray crystallography of allylic fluoride derivative.[9] Notably, while use of (*R*,*R*)-diene ligand yielded (*S*)-allylic fluoride **12** as the major enantiomer, use of (*S*,*S*)-diene ligand afforded (*R*)-**12** as the major enantiomer (Scheme 6). In both cases, only branched allylic fluoride was observed with the linear allylic fluoride byproduct not detected in the reaction.

Scheme 6. Fluorination of racemic substrate using [IrCl(*R*,*R*)-**L**]$_2$ and [IrCl(*S*,*S*)-**L**]$_2$[63]

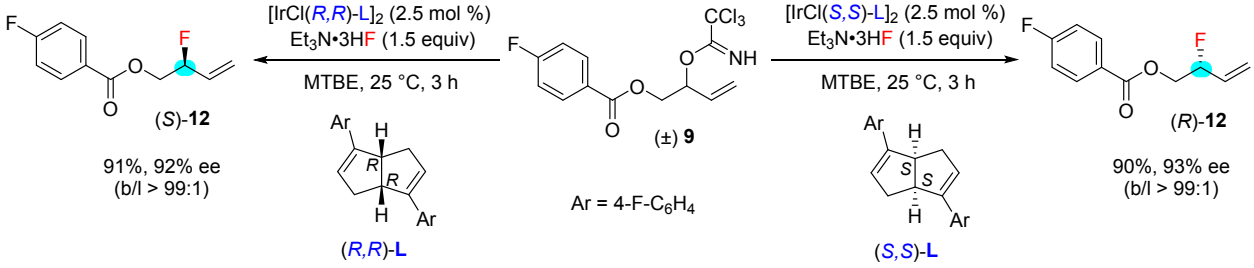

To further validate that the fluorination indeed proceeds through the DYKAT process, the reaction was monitored measuring the enantiomeric excess of the allylic fluoride product **12** and trichloroacetimidate starting material **9**, as a function of time using ^{19}F NMR and chiral HPLC analyses. As illustrated in Figure 3, the enantiomeric excess of the product formed during the reaction remained unchanged as the reaction progressed (90% *ee* at 15% conversion at 20 min → 90% *ee* at 94% conversion at 180 min). Additionally, starting material **9** remained

racemic throughout the course of the reaction. Collectively, this data does not support kinetic resolution of the starting material, but rather suggests that a DYKAT process[55, 61, 64-65] could be operative in the iridium-catalyzed fluorination reaction wherein both enantiomers of starting material **9** convert into a single allylic fluoride product, (*S*)-**12**, with high enantiomeric excess.

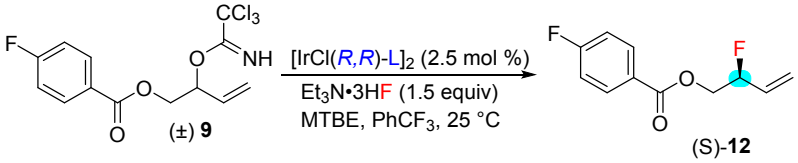

entry	time (min)	conversion (%)	Product **12** (*ee* %)	Starting Material **9** (*ee* %)
1	20	15	90	1
2	40	23	90	1
3	60	33	91	0
4	80	47	88	0
5	100	54	90	-
6	120	67	92	-
7	140	83	90	-
8	160	88	90	-
9	180	94	90	-

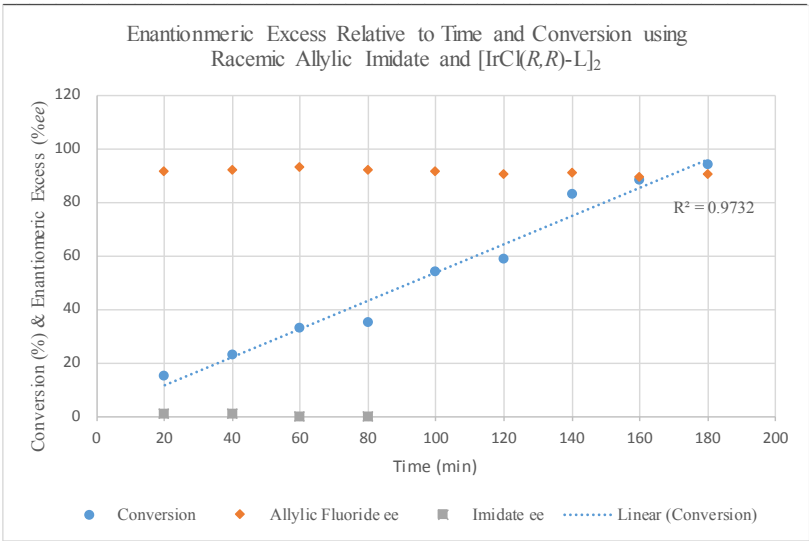

Figure 3. Kinetic profile with racemic allylic trichloroacetimidate **9** using [IrCl(*R*,*R*)-**L**]$_2$

To provide more evidence of a possible DYKAT scenario for the chiral-diene ligated iridium-catalyzed allylic fluorination mechanism, enantioenriched trichloroacetimidates (*S*)-**9** and (*R*)-**9** were submitted to the same [IrCl(*R*,*R*)-**L**]$_2$ catalyst (Scheme 7). A full kinetic profile for (*S*)-**9** with [IrCl(*R*,*R*)-L]$_2$ can be found in Figure S1A). Both reactions gave the same asymmetric product (*S*)-**12** with high enantioselectivity and yield. This result indicates that both reactions proceed through the same chiral iridium complex intermediate. A match/mismatch scenario could explain the slight difference in enantioselectivity and yield.[62]

Scheme 7. Fluorination of (*R*)- and (*S*)-enantioenriched substrates using [IrCl(*R*,*R*)-**L**]$_2$

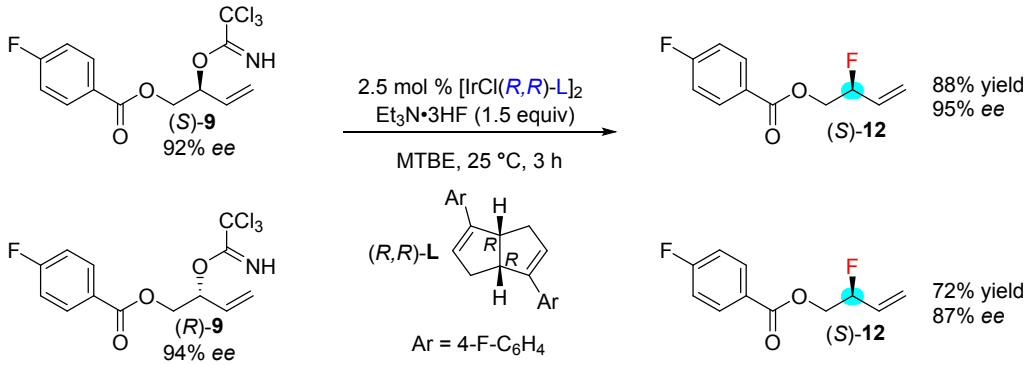

In an attempt to isolate the intermediate in the reaction using chiral diene ligand, the enantioenriched (*R*)-**9** trichloroacetimidate (yellow oil) was reacted with [IrCl(*R*,*R*)-**L**]$_2$ (red solid) to produce a white precipitate, which was presumed to be a π-allyl iridium complex **17**.[66] Unfortunately, crystallization of **17**, which could provide more insight on the π-allyl iridium configuration, was unsuccessful after numerous attempts.[67] Nevertheless, computations (Figure 5) were used to assess the formation of the putative π-allyl intermediates (*vide infra*), which showed low barriers (ca. 11 kcal/mol) for ionization from the chelated complex leading to the corresponding π-allyl iridium intermediates akin to **17**. Moreover, the fluorination of the racemic substrate **9** using a catalytic amount of the presumed π-allyl intermediate **17** led to the formation of allylic fluoride **12** in high yield (85%) and enantioselectivity (90% *ee*) (Scheme 8). This result is comparable to that obtained with the optimized fluorination conditions using the [IrCl(*S*,*S*)-**L**]$_2$ catalyst species (Scheme 6), supporting π-allyl iridium species **17** is catalytically competent.

Scheme 8. Asymmetric fluorination using presumed chiral π-allyl iridium complex as catalyst

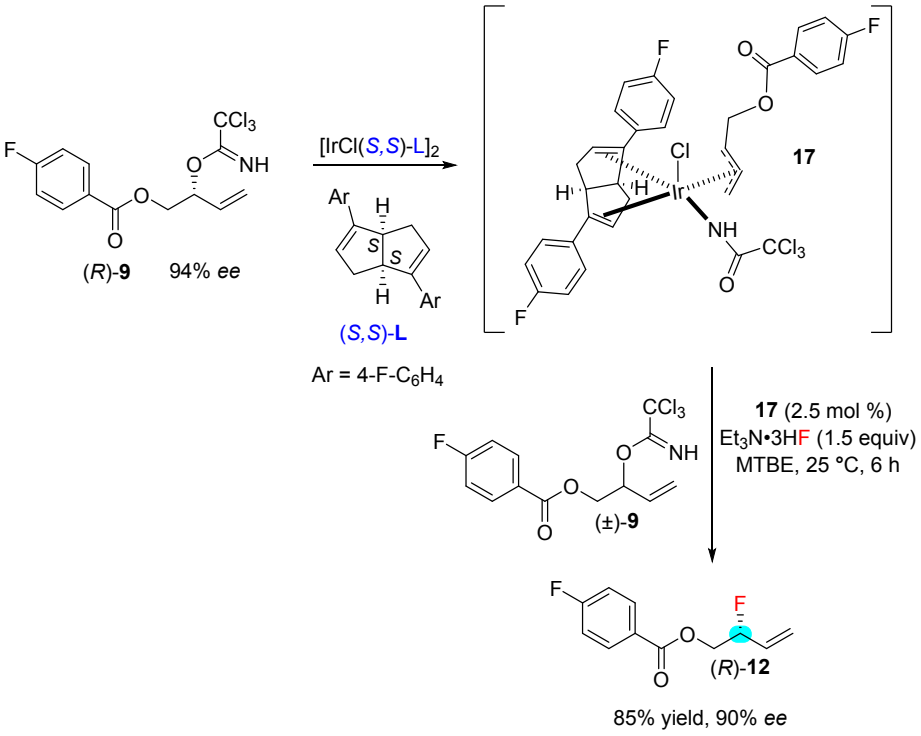

Although the X-ray crystal structure of $[Ir(COD)Cl]_2$ and allylic trichloroacetimidate showed a monomeric pentacoordinated iridium complex, to further confirm the nature of the active catalyst we performed a non-linear test experiment. Optically enriched dimeric catalysts are known to exhibit nonlinear effects, while optically enriched monomeric catalysts provide linear effects.[68] To probe the nature of the active catalyst, we investigated the reaction of racemic allylic trichloroacetimidate **9** with $Et_3N•3HF$ using $[IrCl(R,R)\text{-}\mathbf{L}]_2$ catalyst (**L** = bicyclo[3.3.0]octadiene) of varying enantiomeric purity (Figure 4). Overall, a linear relationship was observed between the product % *ee* and the % *ee* of the catalyst in which increasing the enantiomeric excess of the catalyst resulted in improved enantiomeric excess of the allylic fluoride

product **12**. This result supports a monomeric iridium complex as the active catalyst in the fluorination reaction.

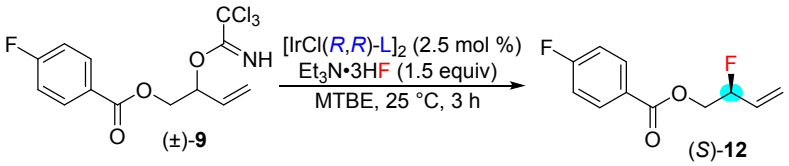

entry	catalyst *ee* (%)	product *ee* (%)
1	0	-6
2	25	32
3	50	48
4	75	71
5	99	92

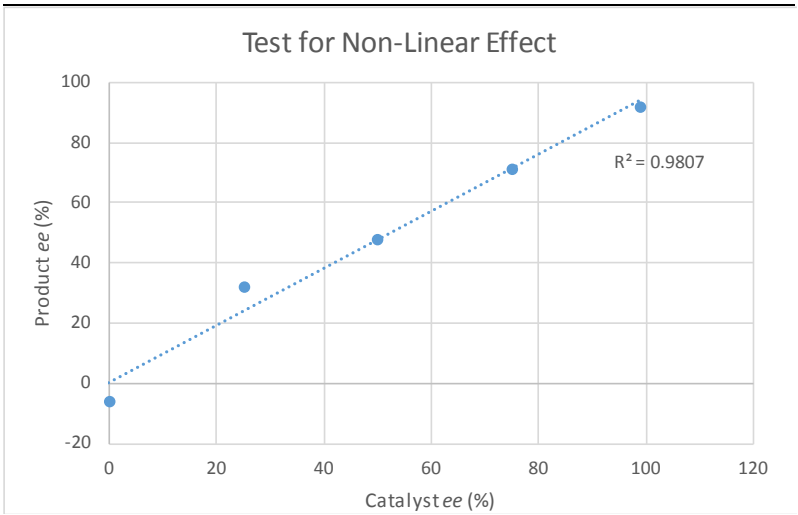

Figure 4. Test for nonlinear effect in the asymmetric iridium-catalyzed allylic fluorination

From the experimental evidence supporting the neutral monomeric nature of the active π-allyl iridium (III) species, computational studies were then employed to examine the various ionization pathways using the chiral (*S*,*S*)-diene (L) ligated iridium catalyst (L = bicyclo[3.3.0]octadiene).[69] As shown in Figure 5 (red), the lowest energy pathway from (*S*)-**II** (R = Me) proceeds via dissociation/re-association of the substrate to form pentacoordinated complex (*S*)-**II'** (i.e., ionization directly from (*S*)-**II** complex is ~5 kcal/mol higher in energy; see Figure S5 in the Supporting Information). Notably, (*S*)-**II'** complex is ca. 6 kcal/mol uphill in energy presumably due to steric interactions between the substrate and the "Cl" group. Nonetheless, from (*S*)-**II'** complex, facile C-O bond breaking via 7-member *bis*-chelated transition state (*S*)-**II'-TS** [relative barrier is 11.3 kcal/mol from (*S*)-**II**] leads directly to the π-allyl iridium intermediate, **I-E$_3$**, downhill in energy by 6 kcal/mol. We also located two distinct pathways for C-O bond breaking that included a [3,3]-sigmatropic rearrangement and 5-member π-*O*-chelation, but these pathways were much higher in energy than the 7-member π-*N*-chelation pathway (see

Figures S15 – S20 in the Supporting Information for information on these pathways); therefore, they were not considered further.

Having established the lowest energy pathway for π-allyl iridium intermediate formation (**I-E$_3$**) from the (*S*)-**II** complex, we next focused on the formation of π-allyl iridium intermediates from (*R*)-**II** (Figure 5, green).[70] Contrary to the (*S*)-**II** complex, (*R*)-**II** favors ionization directly (via transition state (*R*)-**II-TS**) to form π-allyl iridium intermediate **I-E$_1$** with an overall barrier of 11.2 kcal/mol (green-solid).[71] In regard to π-allyl isomerization, the complex **I-E$_1$** can then undergo facile sigma rotation (via **TS-E$_1$-E$_2$**) followed by slippage to form the lower energy π-allyl iridium intermediate **I-E$_2$**. Finally, we also located **TS-*E*$_2$-*E*$_3$** (barrier of 5.2 kcal/mol), which interconverts between **I-E3** and **I-E2** (for information on the conformational search for these transition states, see Figures S21 – S22 in the Supporting Information).

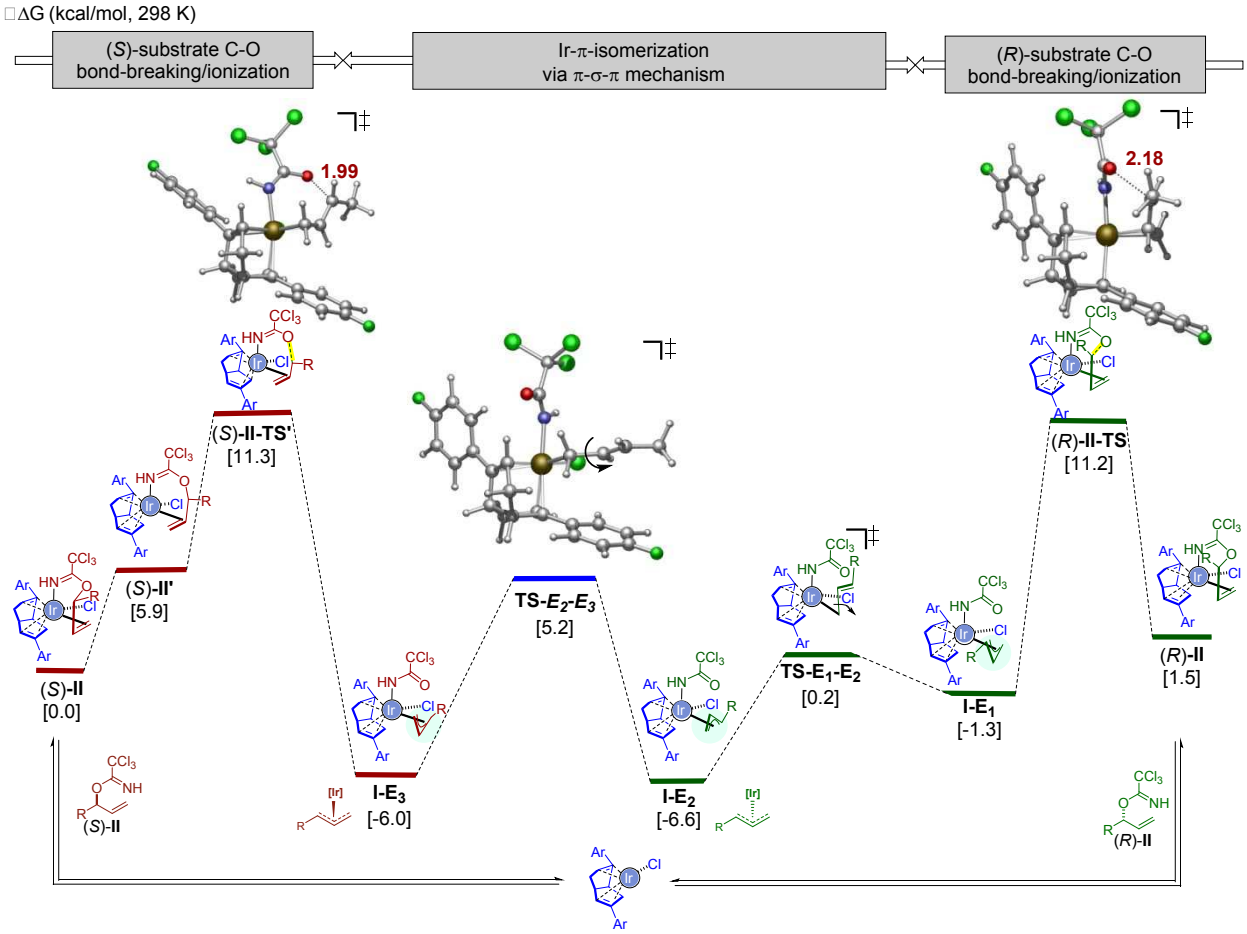

Figure 5. Relative energy for the formation of the π-allyl iridium intermediates from both (*S*)- and (*R*)-allylic trichloroacetimidate (R = Me) using the chiral (*S*,*S*)-diene (L) ligated iridium catalyst (L = bicyclo[3.3.0]octadiene). Free energies (kcal/mol) were computed using B3LYP-D3/6-311+G(d,p)-SDD(Ir)-CPCM(diethylether)//M06/6-31G(d,p)-LANL2DZ(Ir)-CPCM(diethyl

ether) level of theory (For the details on the full pathway, see Figure S23 in the Supporting Information).

Having located the lowest energy pathways for interconversion between (*R*)- and (*S*)-allylic trichloroacetimidate substrates and establishing rapid equilibration among the lowest energy π-allyl iridium intermediates (Figure 5), we next focused on determining the origin of regio- and enantioselectivity.[72] For simplicity, we only discuss nucleophilic attack onto the lowest energy π-allyl iridium intermediates (**I-E$_3$** and **I-E$_2$**) since all others were found to be much higher in energy (see Figure S24 in the Supporting Information). Overall, we found that the lowest energy pathway for iridium-catalyzed allylic fluorination proceeds via *outer-sphere* nucleophilic fluoride attack (see Figure S25 for details on *inner-sphere* attack) onto the lowest energy π-allyl iridium intermediates (Figure 6). The barriers for fluoride attack[73] onto the two lowest energy isomeric π-allyl iridium intermediates leading to linear and branched allylic fluorides are higher in energy (14.3 - 24.9 kcal/mol, Figure 6) than the barriers for isomerization (5.2 kcal/mol) of the π-allyl iridium intermediates (Figure 5). These results strongly support a Curtin-Hammett scenario in which both (*S*)- and (*R*)-allylic tricholoroacetimidates can undergo facile racemization via formation of π-allyl iridium intermediates (i.e., **I-E$_2$** to **I-E$_3$**) followed by regio- and stereodetermining nucleophilic fluoride attack.

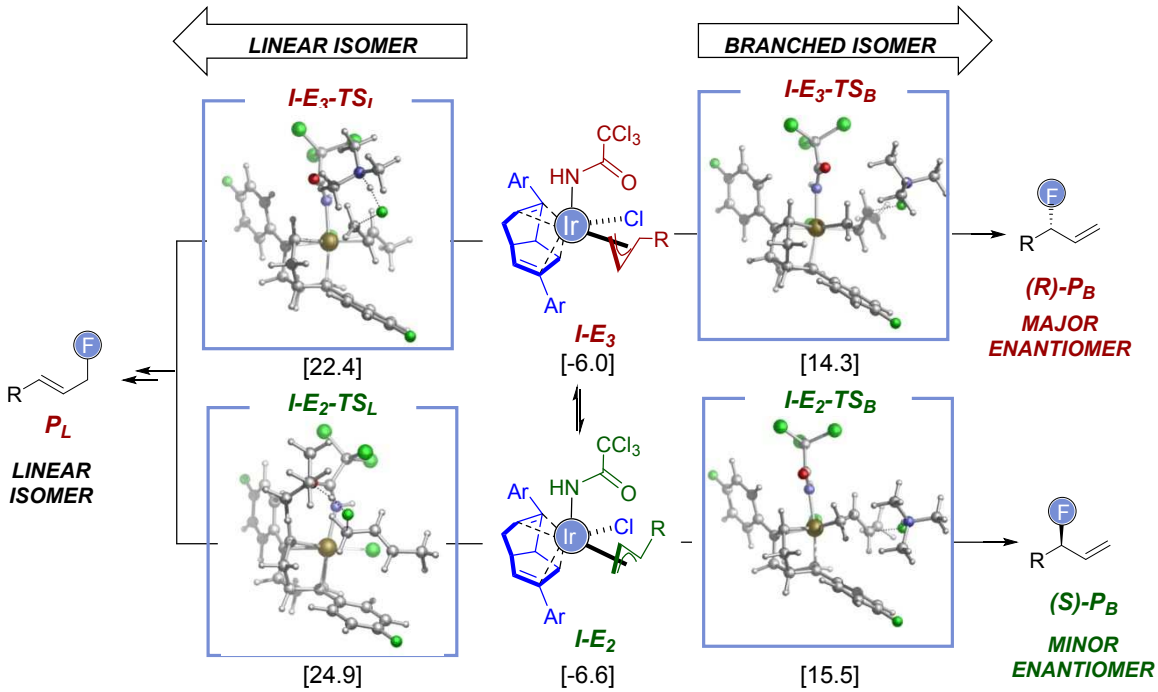

Figure 6. Relative energetics for allylic fluorination of π-allyl iridium intermediates and regioselectivity. Free energies (kcal/mol) were computed using B3LYP-D3/6-311+G(d,p)-

SDD(Ir)-CPCM(diethyl ether)//M06/6-31G(d,p)-LANL2DZ(Ir)-CPCM(diethyl ether) levels of theory.

Moreover, concerning the regioselectivity, the computed barriers for nucleophilic attack at the least substituted carbon (leading to linear products) were significantly higher in energy (8 - 9 kcal/mol) than nucleophilic attack on the most substituted carbon (Figure 6, left versus right). Presumably, the branched transition states benefit from stronger interactions between the developing $\pi_{C=C}$ moiety and the iridium as evident by the shorter Ir-allyl distances in the transition state structures (see Figure S24 in the Supporting Information). Therefore, quantum mechanical calculations predict exclusive formation of branched allylic fluoride products. Collectively, these results are consistent with the experimental regioselectivity in which high branched to linear ratios (b:l >99:1) were observed for a wide range of allylic trichloroacetimidates substrates.

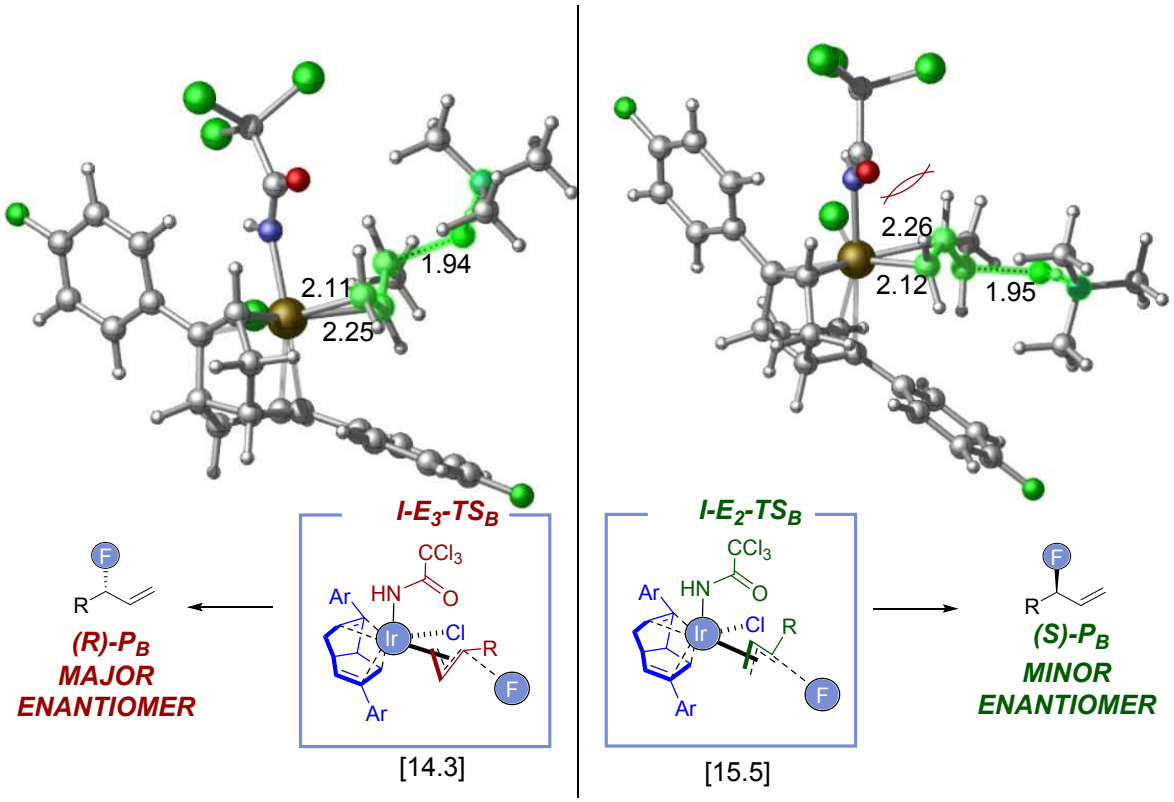

Figure 7. Lowest energy diastereomeric transition states leading to major and minor branched-selective allylic fluorides with relative energies of fluoride addition. Free energies (kcal/mol) were computed using B3LYP-D3/6-311+G(d,p)-SDD(Ir)-CPCM(diethyl ether)//M06/6-31G(d,p)-LANL2DZ(Ir)-CPCM(diethyl ether) levels of theory.

Regarding the enantioselectivity of the branched allylic products, overall, transition state **I-E$_3$-TS$_B$**, which will lead to the experimentally observed enantiomer, is 1.2 kcal/mol lower in

energy than diastereomeric transition state **I-E$_2$-TS$_B$**. This energy difference between the competing diastereomeric transition states is also in reasonable agreement with experiment (%*ee*$_{calc}$ = 76 vs. %*ee*$_{exp}$ = 93; Figure 5) although other methods (UM06 and DLPNO) predict similar results, (M06) %*ee*$_{calc}$ = 96 and (DLPNO) %*ee*$_{calc}$ = 76, respectively (see Figure S31 in the Supporting Information). Closer inspection at the two lowest energy **I-E$_2$-TS$_B$** and **I-E$_3$-TS$_B$** diastereomeric transition states (Figure 7) reveal nearly identical Ir-allyl distances (2.11 and 2.25-2.26 Å), suggesting similar electronic strength[74] of the transition metal fragment and the developing olefin interaction in both transition states. However, in **I-E$_2$-TS$_B$** the allyl group has an unfavorable interaction with the –NHCOCl$_3$ moiety while in **I-E$_3$-TS$_B$** these two groups experience lesser steric interactions.

Scheme 9. Fluorination of enantioenriched deuterium labelled allylic trichloroacetimidates

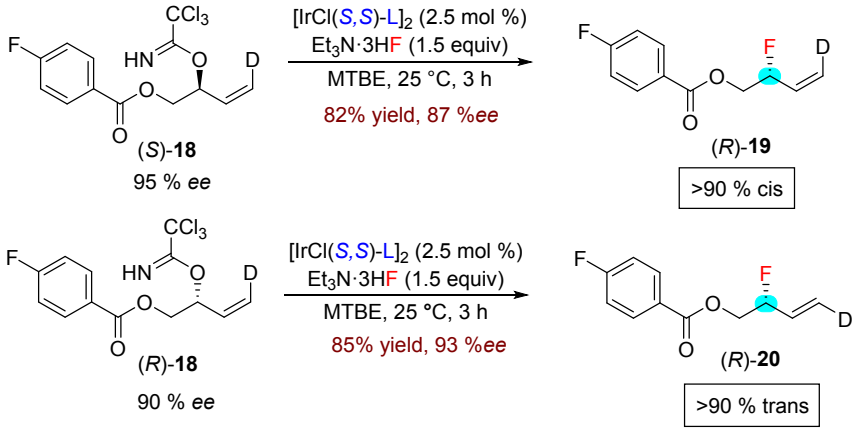

With the establishment of the origin of regioselectivity and enantioselectivity, an additional experiment was pursued to illuminate the nucleophilic attack of the fluoride (outer sphere vs inner sphere). Experiments using deuterium labelled allylic substrates have been employed to probe mechanisms of retention or inversion of stereochemistry.[75-76] The *cis*-alkene deuterium labeled trichloroacetimidate (*S*)-**18** and (*R*)-**18** were synthesized and submitted to the standard fluorination condition using [IrCl(*S*,*S*)-**L**]$_2$ catalyst (Scheme 9). For the (*S*)-**18** substrate using [IrCl(*S*,*S*)-**L**]$_2$, the (*R*)-enantioenriched product **19** was obtained with retention of configuration of the olefin geometry (*cis*). In stark contrast, for the (*R*)-**18** substrate using the [IrCl(*S*,*S*)-**L**]$_2$, the (*R*)-enantioenriched product **20** was obtained with transposition of the deuterium on the terminal alkene (*trans*). Overall, the stereochemistry is consistent with a retention-inversion pathway. Indeed, following the possible mechanism using [IrCl(*S*,*S*)-**L**]$_2$ catalyst (Figure 8); allylic trichloroacetimidate (*S*)-**18**, would go through ionization with retention of stereochemistry and nucleophilic attack with inversion to afford *cis* product **19** without scrambling of deuterium on terminal alkene. On the other hand, allylic trichloroacetimidate (*R*)-**18**, would first proceed through ionization with retention of stereochemistry, the π-allyl iridium intermediate would then undergo isomerization via a π-σ-π mechanism to eventually lead to fluoride nucleophilic attack with inversion to afford *trans*-product **20**.

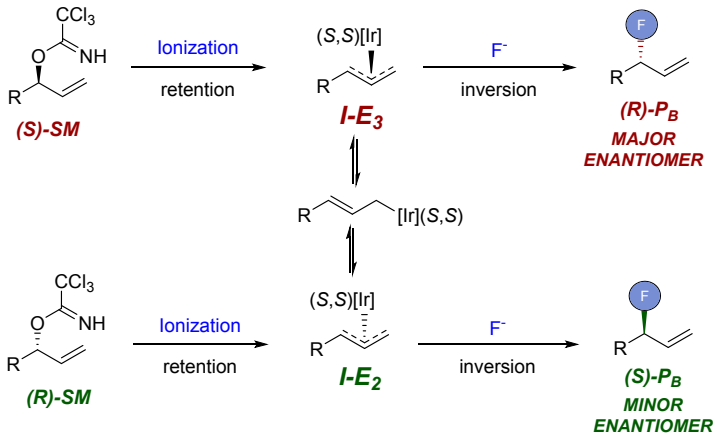

Figure 8. Possible mechanism of Ir-catalyzed DYKAT using [IrCl(*S*,*S*)-**L**]$_2$

CONCLUSION

Our combined experimental and computation studies represent the systematic mechanistic investigation of the diene-ligated iridium catalysts that have been employed in the regio- and enantioselective fluorination of secondary allylic trichloroacetimidates. X-ray crystal structure confirmed the presence of the π-allyl iridium intermediate in the reaction and in combination with computational data suggests that the ionization step would undergo retention of stereochemistry. Furthermore, DFT calculations and deuterium labelled trichloroacetimidate experiments suggest that the nucleophilic attack would undergo regio-determining C-F bond formation proceeding via *outer-sphere* fluoride attack at the more substituted allyl moiety of the η^3-bound π-allyl iridium complex. Taken together, the experimental and computational study supports that fluorination reaction of racemic allylic trichloroacetimidate substrates is likely to occur via a DYKAT process. The importance of the trichloroacetimidate is highlighted through its multiple-purpose role as both a leaving/directing group and a ligand promoting the π–σ–π isomerization leading to a DYKAT process. In future work, we intend to apply the mechanistic findings obtained from these computational and experimental studies to develop more effective catalysts with use of the trichloroacetimidate as the leaving group in other allylic substitutions.

ASSOCIATED CONTENT

Supporting Information

The Supporting Information is available free of charge on the ACS Publications website at DOI:

Full experimental procedures and characterization data for all new compounds (PDF).

X-ray data for π-allyl iridium complex **11** (CIF)

AUTHOR INFORMATION

Corresponding Author: ogs@umd.edu and hmnguyen@wayne.edu

ORCID
Alexandre M. Sorlin: 0000-0002-9589-6131
Jason C. Mixdorf: 0000-0003-3045-5607
Madeline E. Rotella: 0000-0002-7973-2452
Robert T. Martin: 0000-0002-7676-2840
Osvaldo Gutierrez: 0000-0001-8151-7519
Hien M. Nguyen: 0000-0002-7626-8439

Author Contributions: †equal contributions

Notes: The authors declare no competing financial interest.

ACKNOWLEDGMENTS

Financial support from Wayne State University and Carl Johnson Endowed Chair for H.M.N is gratefully acknowledged. J.C.M. thanks the Nuclear Regulatory Commission Program (NRC-HQ-84-14-G-0037) for the graduate fellowship at the University of Iowa. O.G. is grateful to the University of Maryland College Park for start-up funds, and computational resources from UMD DT2 and XSEDE (CHE160082 and CHE160053). We thank Cassandra Ward (the Lumigen Instrument Center) for assistance with X-ray crystallographic analysis.

REFERENCES

1. Attolino, E., *ChemInform Abstract: Trichloroacetimidates: The Great Gift of Carbohydrate Chemistry to Organic Synthesis*. 2013; Vol. 44.

2. Schmidt, R. R.; Michel, J., Facile Synthesis of α- and β-O-Glycosyl Imidates; Preparation of Glycosides and Disaccharides. *Angew. Chem. Int. Ed. Engl.* **1980,** *19* (9), 731-732.

3. Schmidt, R. R., New Methods for the Synthesis of Glycosides and Oligosaccharides—Are There Alternatives to the Koenigs-Knorr Method? [New Synthetic Methods (56)]. *Angew. Chem. Int. Ed. Engl.* **1986,** *25* (3), 212-235.

4. Schmidt, R. R.; Zhu, X., Glycosyl Trichloroacetimidates. In *Glycoscience: Chemistry and Chemical Biology*, Fraser-Reid, B. O.; Tatsuta, K.; Thiem, J., Eds. Springer Berlin Heidelberg: Berlin, Heidelberg, 2008; pp 451-524.

5. Overman, L. E., Thermal and mercuric ion catalyzed [3,3]-sigmatropic rearrangement of allylic trichloroacetimidates. 1,3 Transposition of alcohol and amine functions. *J. Am. Chem. Soc.* **1974,** *96* (2), 597-599.

6. Anderson, C. E.; Overman, L. E., Catalytic Asymmetric Rearrangement of Allylic Trichloroacetimidates. A Practical Method for Preparing Allylic Amines and Congeners of High Enantiomeric Purity. *J. Am. Chem. Soc.* **2003,** *125* (41), 12412-12413.

7. Arnold, J. S.; Zhang, Q.; Nguyen, H. M., Transition-Metal-Catalyzed Allylic Substitutions of Trichloroacetimidates. *Eur. J. Org. Chem.* **2014,** *2014* (23), 4925-4948.

8. Topczewski, J. J.; Tewson, T. J.; Nguyen, H. M., Iridium-Catalyzed Allylic Fluorination of Trichloroacetimidates. *J. Am. Chem. Soc.* **2011,** *133* (48), 19318-19321.

9. Mixdorf, J. C.; Sorlin, A. M.; Zhang, Q.; Nguyen, H. M., Asymmetric Synthesis of Allylic Fluorides via Fluorination of Racemic Allylic Trichloroacetimidates Catalyzed by a Chiral Diene-Iridium Complex. *ACS Catal.* **2018,** *8* (2), 790-801.

10. Klimko, P.; Hellberg, M.; McLaughlin, M.; Sharif, N.; Severns, B.; Williams, G.; Haggard, K.; Liao, J., 15-Fluoro prostaglandin FP agonists: a new class of topical ocular hypotensives. *Bioorg. Med. Chem.* **2004,** *12* (13), 3451-3469.

11. Bannai, K.; Toru, T.; Ōba, T.; Tanaka, T.; Okamura, N.; Watanabe, K.; Hazato, A.; Kurozumi, S., Synthesis of chemically stable prostacyclin analogs. *Tetrahedron* **1983,** *39* (22), 3807-3819.

12. Karen, V. P.; Ying, K. Y.; Bernard, Y. A.; Sunil, N., Vitamin D Receptor as a Drug Discovery Target. *Mini-Rev. Med. Chem.* **2003,** *3* (3), 193-204.

13. Marchiani, S.; Bonaccorsi, L.; Ferruzzi, P.; Crescioli, C.; Muratori, M.; Adorini, L.; Forti, G.; Maggi, M.; Baldi, E., The vitamin D analogue BXL-628 inhibits growth factor-stimulated proliferation and invasion of DU145 prostate cancer cells. *J. Cancer Res. Clin. Oncol.* **2006,** *132* (6), 408-416.

14. Maggi, M.; Crescioli, C.; Morelli, A.; Colli, E.; Adorini, L., Pre-clinical evidence and clinical translation of benign prostatic hyperplasia treatment by the vitamin D receptor agonist BXL-628 (Elocalcitol). *J. Endocrinol. Invest.* **2006,** *29* (7), 665-674.

15. Adorini, L.; Penna, G.; Amuchastegui, S.; Cossetti, C.; Aquilano, F.; Mariani, R.; Fibbi, B.; Morelli, A.; Uskokovic, M.; Colli, E.; Maggi, M., Inhibition of prostate growth and inflammation by the vitamin D receptor agonist BXL-628 (elocalcitol). *J. Steroid Biochem. Mol. Biol.* **2007,** *103* (3), 689-693.

16. Stehouwer, J. S.; Daniel, L. M.; Chen, P.; Voll, R. J.; Williams, L.; Plott, S. J.; Votaw, J. R.; Owens, M. J.; Howell, L.; Goodman, M. M., Synthesis, Fluorine-18 Radiolabeling, and Biological Evaluation of N-((E)-4-Fluorobut-2-en-1-yl)-2β-carbomethoxy-3β-(4′-halophenyl)nortropanes: Candidate Radioligands for In Vivo Imaging of the Brain Dopamine Transporter with Positron Emission Tomography. *J. Med. Chem.* **2010,** *53* (15), 5549-5557.

17. Pacheco, M. C.; Purser, S.; Gouverneur, V., The Chemistry of Propargylic and Allylic Fluorides. *Chem. Rev.* **2008,** *108* (6), 1943-1981.

18. Yang, X.; Wu, T.; Phipps, R. J.; Toste, F. D., Advances in Catalytic Enantioselective Fluorination, Mono-, Di-, and Trifluoromethylation, and Trifluoromethylthiolation Reactions. *Chem. Rev.* **2015,** *115* (2), 826-870.

19. Hollingworth, C.; Hazari, A.; Hopkinson, M. N.; Tredwell, M.; Benedetto, E.; Huiban, M.; Gee, A. D.; Brown, J. M.; Gouverneur, V., Palladium-Catalyzed Allylic Fluorination. *Angew. Chem. Int. Ed.* **2011,** *50* (11), 2613-2617.

20. Benedetto, E.; Tredwell, M.; Hollingworth, C.; Khotavivattana, T.; Brown, J. M.; Gouverneur, V., Regio- and stereoretentive synthesis of branched, linear (E)- and (Z)-allyl fluorides from allyl carbonates under Ir-catalysis. *Chem. Sci.* **2013,** *4* (1), 89-96.

21. Lauer, A. M.; Wu, J., Palladium-Catalyzed Allylic Fluorination of Cinnamyl Phosphorothioate Esters. *Org. Lett.* **2012,** *14* (19), 5138-5141.

22. Braun, M.-G.; Katcher, M. H.; Doyle, A. G., Carbofluorination via a palladium-catalyzed cascade reaction. *Chem. Sci.* **2013,** *4* (3), 1216-1220.

23. Zhang, Q.; Nguyen, H. M., Rhodium-catalyzed regioselective opening of vinyl epoxides with Et3N·3HF reagent – formation of allylic fluorohydrins. *Chem. Sci.* **2014,** *5* (1), 291-296.

24. Braun, M.-G.; Doyle, A. G., Palladium-Catalyzed Allylic C–H Fluorination. *J. Am. Chem. Soc.* **2013,** *135* (35), 12990-12993.

25. Zhang, Z.; Wang, F.; Mu, X.; Chen, P.; Liu, G., Copper-Catalyzed Regioselective Fluorination of Allylic Halides. *Angew. Chem. Int. Ed.* **2013,** *52* (29), 7549-7553.

26. Katcher, M. H.; Doyle, A. G., Palladium-Catalyzed Asymmetric Synthesis of Allylic Fluorides. *J. Am. Chem. Soc.* **2010,** *132* (49), 17402-17404.

27. Katcher, M. H.; Sha, A.; Doyle, A. G., Palladium-Catalyzed Regio- and Enantioselective Fluorination of Acyclic Allylic Halides. *J. Am. Chem. Soc.* **2011,** *133* (40), 15902-15905.

28. Zhu, J.; Tsui, G. C.; Lautens, M., Rhodium-Catalyzed Enantioselective Nucleophilic Fluorination: Ring Opening of Oxabicyclic Alkenes. *Angew. Chem. Int. Ed.* **2012,** *51* (49), 12353-12356.

29. Zhang, Q.; Stockdale, D. P.; Mixdorf, J. C.; Topczewski, J. J.; Nguyen, H. M., Iridium-Catalyzed Enantioselective Fluorination of Racemic, Secondary Allylic Trichloroacetimidates. *J. Am. Chem. Soc.* **2015,** *137* (37), 11912-11915.

30. Butt, N. A.; Zhang, W., Transition metal-catalyzed allylic substitution reactions with unactivated allylic substrates. *Chem. Soc. Rev.* **2015,** *44* (22), 7929-7967.

31. Trost, B. M.; Crawley, M. L., Asymmetric Transition-Metal-Catalyzed Allylic Alkylations: Applications in Total Synthesis. *Chem. Rev.* **2003,** *103* (8), 2921-2944.

32. Trost, B. M.; Van Vranken, D. L., Asymmetric Transition Metal-Catalyzed Allylic Alkylations. *Chem. Rev.* **1996,** *96* (1), 395-422.

33. Gansäuer, A.; Justicia, J.; Rosales, A.; Worgull, D.; Rinker, B.; Cuerva, J. M.; Oltra, J. E., Transition-Metal-Catalyzed Allylic Substitution and Titanocene-Catalyzed Epoxypolyene Cyclization as a Powerful Tool for the Preparation of Terpenoids. *Eur. J. Org. Chem.* **2006,** *2006* (18), 4115-4127.

34. Poli, G.; Prestat, G.; Liron, F.; Kammerer-Pentier, C.; Kleimark, J.; Norrby, P.-O.; Milhau, L.; Guiry, P. J.; Liu, W.-B.; Xia, J.-B.; You, S.-L.; Moberg, C.; Langlois, J.-B.; Alexakis, A.; Begouin, J.-M.; Klein, J. E. M. N.; Weickmann, D.; Plietker, B.; Trost, B. M.; Crawley, M. L., *Transition Metal Catalyzed Enantioselective Allylic Substitution in Organic Synthesis*. Springer-Verlag Berlin Heidelberg: 2012; Vol. 38, p 348.

35. Katcher, M. H.; Norrby, P.-O.; Doyle, A. G., Mechanistic Investigations of Palladium-Catalyzed Allylic Fluorination. *Organometallics* **2014,** *33* (9), 2121-2133.

36. Hayashi, T.; Kawatsura, M.; Uozumi, Y., Regio- and enantio-selective allylic alkylation catalysed by a chiral monophosphine–palladium complex. *Chem. Commun.* **1997,** (6), 561-562.

37. Helmchen, G.; Pfaltz, A., PhosphinooxazolinesA New Class of Versatile, Modular P,N-Ligands for Asymmetric Catalysis. *Acc. Chem. Res.* **2000,** *33* (6), 336-345.

38. Aakermark, B.; Vitagliano, A., Reactivity and syn-anti isomerization of (.eta.3-geranyl)- and (.eta.3-neryl)palladium complexes. Evidence for electronic control of the regiochemistry of nucleophilic addition. *Organometallics* **1985,** *4* (7), 1275-1283.

39. Trost, B. M.; Dietsche, T. J.; Fullerton, T. J., New synthetic reactions. Chemospecificity of allylic alkylation. *J. Org. Chem.* **1974,** *39* (5), 737-738.

40. Madrahimov, S. T.; Hartwig, J. F., Origins of Enantioselectivity during Allylic Substitution Reactions Catalyzed by Metallacyclic Iridium Complexes. *J. Am. Chem. Soc.* **2012,** *134* (19), 8136-8147.

41. Rössler, S. L.; Petrone, D. A.; Carreira, E. M., Iridium-Catalyzed Asymmetric Synthesis of Functionally Rich Molecules Enabled by (Phosphoramidite,Olefin) Ligands. *Acc. Chem. Res.* **2019**.

42. Cheng, Q.; Tu, H.-F.; Zheng, C.; Qu, J.-P.; Helmchen, G.; You, S.-L., Iridium-Catalyzed Asymmetric Allylic Substitution Reactions. *Chem. Rev.* **2019,** *119* (3), 1855-1969.

43. Cossi, M.; Rega, N.; Scalmani, G.; Barone, V., Energies, structures, and electronic properties of molecules in solution with the C-PCM solvation model. *J. Comput. Chem.* **2003,** *24* (6), 669-681.

44. Takano, Y.; Houk, K. N., Benchmarking the Conductor-like Polarizable Continuum Model (CPCM) for Aqueous Solvation Free Energies of Neutral and Ionic Organic Molecules. *J. Chem. Theory Comput.* **2005,** *1* (1), 70-77.

45. Hay, P. J.; Wadt, W. R., Ab initio effective core potentials for molecular calculations. Potentials for the transition metal atoms Sc to Hg. *The Journal of Chemical Physics* **1985,** *82* (1), 270-283.

46. Wadt, W. R.; Hay, P. J., Ab initio effective core potentials for molecular calculations. Potentials for main group elements Na to Bi. *J. Chem. Phys.* **1985,** *82* (1), 284-298.

47. Hay, P. J.; Wadt, W. R., Ab initio effective core potentials for molecular calculations. Potentials for K to Au including the outermost core orbitals. *J. Chem. Phys.* **1985,** *82* (1), 299-310.

48. Sperger, T.; Sanhueza, I. A.; Kalvet, I.; Schoenebeck, F., Computational Studies of Synthetically Relevant Homogeneous Organometallic Catalysis Involving Ni, Pd, Ir, and Rh: An Overview of Commonly Employed DFT Methods and Mechanistic Insights. *Chem. Rev.* **2015,** *115* (17), 9532-9586.

49. Similarly, a preference for bidentate coordination was also observed with use of both allylic (*R*)- and (*S*)-trichloroacetimidate substrates using chiral (*S,S*)-diene ligand 5 (see Figure S1 in the Supporting Information).

50. Rössler, S. L.; Krautwald, S.; Carreira, E. M., Study of Intermediates in Iridium–(Phosphoramidite,Olefin)-Catalyzed Enantioselective Allylic Substitution. *J. Am. Chem. Soc.* **2017,** *139* (10), 3603-3606.

51. DFT calculations were also performed for the coordination of chiral diene ligated ligated iridium complex to the allylic trichloroacetimidate.

52. Straub, B. F., Organotransition Metal Chemistry. From Bonding to Catalysis. Edited by John F. Hartwig. *Angew. Chem. Int. Ed.* **2010,** *49* (42), 7622-7622.

53. Tsuji, J., New general synthetic methods involving π-allylpalladium complexes as intermediates and neutral reaction conditions. *Tetrahedron* **1986,** *42* (16), 4361-4401.

54. Racemic 17 was subjected to the optimized enantioselective conditions leading to nearly racemic product (2% *ee*).

55. Hartwig, J. F.; Stanley, L. M., Mechanistically Driven Development of Iridium Catalysts for Asymmetric Allylic Substitution. *Acc. Chem. Res.* **2010,** *43* (12), 1461-1475.

56. Takeuchi, R.; Kashio, M., Iridium Complex-Catalyzed Allylic Alkylation of Allylic Esters and Allylic Alcohols: Unique Regio- and Stereoselectivity. *J. Am. Chem. Soc.* **1998,** *120* (34), 8647-8655.

57. Faller, J. W.; Thomsen, M. E.; Mattina, M. J., Organometallic conformational equilibriums. X. Steric factors and their mechanistic implications in .pi.-allyl(amine)chloropalladium(II) complexes. *J. Am. Chem. Soc.* **1971,** *93* (11), 2642-2653.

58. Tsutsui, M.; Courtney, A., σ-π Rearrangements of Organotransition Metal Compounds in Homogeneous Catalysis. In *Fundamental Research in Homogeneous Catalysis: Volume 2*, Ishii, Y.; Tsutsui, M., Eds. Springer US: Boston, MA, 1978; pp 125-158.

59. Trost, B. M.; Toste, F. D., Regio- and Enantioselective Allylic Alkylation of an Unsymmetrical Substrate: A Working Model. *J. Am. Chem. Soc.* **1999,** *121* (19), 4545-4554.

60. Bartels, B.; García-Yebra, C.; Rominger, F.; Helmchen, G., Iridium-Catalysed Allylic Substitution: Stereochemical Aspects and Isolation of IrIII Complexes Related to the Catalytic Cycle. *Eur. J. Inorg. Chem.* **2002,** *2002* (10), 2569-2586.

61. Steinreiber, J.; Faber, K.; Griengl, H., De-racemization of Enantiomers versus De-epimerization of Diastereomers—Classification of Dynamic Kinetic Asymmetric Transformations (DYKAT). *Chem. Eur. J.* **2008,** *14* (27), 8060-8072.

62. Faber, K., Non-Sequential Processes for the Transformation of a Racemate into a Single Stereoisomeric Product: Proposal for Stereochemical Classification. *Chem. Eur. J.* **2001,** *7* (23), 5004-5010.

63. To establish the absolute stereochemistry of the desired allylic fluoride products, compound 12 was subjected to cross-metathesis with 4-bromostyrene in the presence of Hoveyda-Grubbs II catalyst. The internal allylic fluoride was isolated as a crystalline solid with almost no loss of enantiomeric purity and its absolute stereochemistry was then confirmed by x-ray analysis.

64. You, S.-L.; Zhu, X.-Z.; Luo, Y.-M.; Hou, X.-L.; Dai, L.-X., Highly Regio- and Enantioselective Pd-Catalyzed Allylic Alkylation and Amination of Monosubstituted Allylic Acetates with Novel Ferrocene P,N-Ligands. *J. Am. Chem. Soc.* **2001,** *123* (30), 7471-7472.

65. Lafrance, M.; Roggen, M.; Carreira, E. M., Direct, Enantioselective Iridium-Catalyzed Allylic Amination of Racemic Allylic Alcohols. *Angew. Chem. Int. Ed.* **2012,** *51* (14), 3470-3473.

66. Madrahimov, S. T.; Markovic, D.; Hartwig, J. F., The Allyl Intermediate in Regioselective and Enantioselective Iridium-Catalyzed Asymmetric Allylic Substitution Reactions. *J. Am. Chem. Soc.* **2009,** *131* (21), 7228-7229.

67. Exchanging fluoride to bromide on the phenyl ring of the benzoyl group also did not lead to successful crystallization.

68. Guillaneux, D.; Zhao, S.-H.; Samuel, O.; Rainford, D.; Kagan, H. B., Nonlinear Effects in Asymmetric Catalysis. *J. Am. Chem. Soc.* **1994,** *116* (21), 9430-9439.

69. Raskatov, J. A.; Spiess, S.; Gnamm, C.; Brödner, K.; Rominger, F.; Helmchen, G., Ir-Catalysed Asymmetric Allylic Substitutions with Cyclometalated (Phosphoramidite)Ir Complexes—Resting States, Catalytically Active (π-Allyl)Ir Complexes and Computational Exploration. *Chem. Eur. J.* **2010,** *16* (22), 6601-6615.

70. Bhaskararao, B.; Sunoj, R. B., Origin of Stereodivergence in Cooperative Asymmetric Catalysis with Simultaneous Involvement of Two Chiral Catalysts. *J. Am. Chem. Soc.* **2015,** *137* (50), 15712-15722.

71. Here, "E" in the labelling scheme stands for the trans isomer of the allylic moiety alkene.

72. Madrahimov, S. T.; Li, Q.; Sharma, A.; Hartwig, J. F., Origins of Regioselectivity in Iridium Catalyzed Allylic Substitution. *J. Am. Chem. Soc.* **2015,** *137* (47), 14968-14981.

73. For information on the fluoride source and the choice of the basis set for the F atom used in the computational studies, see Figure S26-S30 in the Supporting Information.

74. See Figure S32 in the Supporting Information for a distortion-interaction analysis on this system to gain insights into the energetic difference between.

75. Hughes, D. L.; Lloyd-Jones, G. C.; Krska, S. W.; Gouriou, L.; Bonnet, V. D.; Jack, K.; Sun, Y.; Mathre, D. J.; Reamer, R. A., Mechanistic studies of the molybdenum-catalyzed asymmetric alkylation reaction. *Proc. Natl. Acad. Sci. U. S. A.* **2004,** *101* (15), 5379-5384.

76. Gouriou, L.; Lloyd-Jones, G. C.; Vyskočil, Š.; Kočovský, P., 2H-quadrupolar coupling-based analysis of stereochemical and regiochemical memory in the Pd-catalysed allylic alkylation of iso-cinnamyl type substrates employing the chiral monophosphine ligands ‘MOP’ and ‘MAP’. *J. Organomet. Chem.* **2003,** *687* (2), 525-537.

Table of Contents